Microsecond Protein Folding Kinetics from Native-State Hydrogen Exchange[†]

Cammon B. Arrington and Andrew D. Robertson*

Department of Biochemistry, The University of Iowa, Iowa City, Iowa 52242

Received April 15, 1997; Revised Manuscript Received May 29, 1997[⊗]

ABSTRACT: Native-state amide proton (NH) exchange in turkey ovomucoid third domain (OMTKY3) has been used to determine rates of unfolding and folding at the 13 most slowly exchanging residues. Ten of the 13 NHs have previously been demonstrated to exchange via complete unfolding of OMTKY3 while the remaining three exchange more slowly than expected on the basis of thermal stability alone [Swint-Kruse, L., & Robertson, A. D. (1996) *Biochemistry 35*, 171−180]. Rates of unfolding and folding have been determined by monitoring NH exchange over a range of pH where (1) the free energy of unfolding for third domain, about 7 kcal/mol, is insensitive to pH and (2) the mechanism of exchange changes from one governed by a rapid equilibrium preceding the chemistry of exchange (i.e., EX2 exchange) to one where exchange is limited by the rate of unfolding (i.e., EX1 exchange). The pH dependence of exchange has then been fit to a two-state model to obtain the unfolding and folding rates. Unfolding rates at these 13 NHs in native third domain range from 0.003 to ≥ 0.03 s^{-1}. No correlation is observed between opening rates and the free energies measured at the same NHs: for example, the slowest and most rapid opening rates occur at Leu 23 and Asn 33, respectively, and these two NHs show very similar free energies of 6.7 and 6.9 kcal/mol, respectively. In contrast, folding rates show a positive correlation ($R^2 = 0.90$) with free energies, the most rapid folding occurring at the sites with the largest free energies. Folding rates are most rapid, 10^3-10^4 s^{-1}, in the middle of the helix, intermediate rates of around 10^3 s^{-1} are found in the remainder of the helix and through much of the β-sheet, and the slowest folding, 10^2-10^3 s^{-1}, occurs at the juncture between the helix and sheet. Overall, NH exchange from native proteins provides remarkable structural and temporal precision for measuring very rapid conformational fluctuations.

Much of the current investigation into the mechanism of protein folding is guided by two recent developments in the field: the experimental observation of very rapid folding (*1*−*4*) and the realization that folding is probably a structurally complex process involving ensembles of conformations rather than distinct pathways (*5*). Key events in protein folding can occur on a submillisecond time scale, and in some instances, folding may go to completion in as little as 100 μs (*6*). Experiments to detect these rapid events are yielding a wealth of information regarding the kinetics of folding but generally report on either macroscopic properties of the protein or a very small subset of the possible noncovalent interactions during folding. In contrast, rapid mixing experiments involving amide hydrogen (NH) exchange provide rich structural detail during folding and unfolding reactions, but important events are occurring in the millisecond dead times for these experiments (*7, 8*). We report here a relatively simple experimental method that provides structural detail on a submillisecond time scale: native-state NH exchange at alkaline pH.

Native-state NH exchange experiments are typically performed by dissolving native protein into D_2O[1] and then monitoring the disappearance of the NH resonances by ^1H NMR spectroscopy. The slowing of NH exchange in native proteins relative to peptides is most often modeled by the two-state mechanism (*9*):

$$\text{NH(closed)} \underset{k_{cl}}{\overset{k_{op}}{\rightleftharpoons}} \text{NH(open)} \xrightarrow{k_{ch}} \text{exchanged} \qquad (1)$$

where k_{op} is the rate at which a given NH is exposed to solvent, k_{cl} is the closing or folding rate, and k_{ch} is the rate of NH exchange in model peptides (*10*). The reaction depicted in eq 1 consists of an equilibrium between a closed conformation, from which exchange cannot occur, and an open conformation from which exchange occurs with the model peptide rate, k_{ch}.

Specific "two-process" models for NH exchange have been derived from eq 1 in order to explore the possibility that two processes, global unfolding and local fluctuations, are sufficient to describe exchange at all NHs in native proteins (*11, 12*). However, in this paper we focus on NHs where exchange appears to be governed by global unfolding alone. Under native-state conditions, where $k_{op} \ll k_{cl}$, and assuming that the concentration of "NH(open)" is in a steady state, the observed rate of exchange is described by the equation (*9*):

$$k_{obs} = (k_{op}k_{ch})/(k_{cl} + k_{ch}) \qquad (2)$$

Equation 2 is often simplified by consideration of two

[†] This work was supported by the National Institutes of Health (Grant GM46849).

* Corresponding author. Fax: (319) 335-9570. E-mail: andy-robertson@uiowa.edu.

[1] Abbreviations: $\Delta G°$, change in Gibbs free energy for protein unfolding; *a*, amplitude of an exchange decay curve; *c*, a constant value that describes the offset of the exchange curve from zero; D_2O, deuterium oxide; EX1, mechanism of hydrogen exchange in which k_{obs} equals k_{op}; EX2, mechanism of hydrogen exchange in which k_{obs} equals $k_{ch}(k_{op}/k_{cl})$; FID, free induction decay; *h*, normalized height of an amide proton peak; k_{cl}, closing or folding rate; k_{ch}, exchange rate in model peptides; k_{obs}, observed exchange rate; k_{op}, opening or unfolding rate; NH, amide hydrogen; NMR, nuclear magnetic resonance; OMTKY3, turkey ovomucoid third domain; *R*, universal gas constant; *T*, temperature; *t*, time in minutes; τ, time constant.

[⊗] Abstract published in *Advance ACS Abstracts,* July 1, 1997.

S0006-2960(97)00872-6 CCC: $14.00

possible limiting cases. The first is EX2 exchange, where $k_{cl} >> k_{ch}$. Under such conditions, eq 2 simplifies to the equation:

$$k_{obs} = k_{ch}(k_{op}/k_{cl}) \quad (3)$$

In principle, EX2 exchange is thus capable of providing measures of conformational equilibria (k_{op}/k_{cl}) in native proteins. The smallest values for k_{ch} occur at about pH 3, so EX2 exchange is typically observed at acidic pH. Previous studies have demonstrated that a subset of the slowest exchanging NHs provides accurate measures of unfolding equilibria in native proteins (*13*−*21*). For this subset of slow exchangers, the model for NH exchange depicted in eq 1 is accurate.

The second limiting case occurs when $k_{ch} \gg k_{cl}$, which is called EX1 exchange. Equation 2 then simplifies to

$$k_{obs} = k_{op} \quad (4)$$

thus permitting direct determination of the rate of opening. EX1 exchange has been detected in a number of proteins, where experimental conditions have increased k_{ch} by raising the pH (*22*−*25*) or decreased k_{cl} by either raising the temperature (*26*) or adding denaturant (*16*, *27*).

Some investigators have recognized that a combination of EX2 and EX1 exchange at the slowest exchanging NHs should permit calculation of the rate of folding (i.e., closing, k_{cl}) (*22*−*24*, *28*), but the full potential of this idea has not yet been realized experimentally. We show that a comprehensive analysis of the pH dependence of native-state NH exchange in turkey ovomucoid third domain (OMTKY3) yields very rapid closing rates at multiple sites distributed throughout much of its structure.

MATERIALS AND METHODS

The purification of OMTKY3 has been described previously (*20*). Exchange samples were prepared by adjusting aliquots of pure OMTKY3 in H_2O to the desired experimental pH with potassium hydroxide. Protein solutions were then lyophilized to a constant weight. Exchange buffers, consisting of 10 mM glycine and 10 mM glycylglycine in D_2O, were also preadjusted to the desired experimental pH by addition of sodium deuterioxide (Cambridge Isotope Laboratories). The final concentration of buffered OMTKY3 was approximately 2 mM for each experiment. Sample pH was measured after each experiment as described previously (*20*). The pH values reported herein are for D_2O solutions and have not been corrected for isotope effects.

NMR spectrometer specifications have been described previously (*20*). The spectrometer's variable temperature controller was calibrated to 30 °C using a methanol standard (uncertainty ± 0.5 °C) (*29*). Exchange was initiated by mixing lyophilized OMTKY3 with D_2O buffer. Experimental dead times (i.e., time between dissolving protein to the start of data acquisition) were between 5 and 10 min. Each FID was the sum of 16 transients consisting of 8000 time-domain data points. The spectral width was 6000 Hz and the recycle delay was 1.5 s. Total data acquisition time for each FID was 38 s, and FIDs were acquired at 20−30 time points for most experiments.

NH resonance peak heights were normalized to two nonexchanging aromatic signals. Hydrogen exchange rates were determined by fitting normalized peak height versus time (*30*) to the equation:

$$h = a \exp(-k_{obs}t) + c \quad (5)$$

where h is the normalized peak height, a is the amplitude of the exchange curve, k_{obs} is the observed hydrogen exchange rate constant, t is the time in minutes, and c is a constant. Rates were only determined for NHs where resonance intensities were above baseline for at least four time points.

RESULTS

How can native-state NH exchange, which may take anywhere from minutes to days to go to completion, be used to measure fast events in protein folding? The approach takes advantage of exchange data obtained under solution conditions ranging from low pH, where EX2 exchange provides equilibrium constants (i.e., k_{op}/k_{cl}), to alkaline pH, where EX1 exchange provides estimates for k_{op} (i.e., the rate of unfolding). These data are thus sufficient for calculation of k_{cl}, the folding rates (*28*). In the present studies of OMTKY3, exchange rates obtained over a wide range of pH have been fit to eq 2 to determine values for k_{op} and k_{cl} at individual NHs.

One assumption in this analysis is that k_{op} and k_{cl} values are not changing as the pH is raised from 6 to pH 10. The best evidence in this regard is that the stability of OMTKY3 shows little change from pH 6 to pH 10, as indicated by the following observations. First, the midpoint for thermal denaturation of OMTKY3 in H_2O at both pH 9 and pH 10 is 80 °C (Forsyth and Robertson, unpublished results), which is only 5° less than at pH 5 (*31*). This corresponds to a decrease of about 0.5 kcal/mol in $\Delta G°$ for unfolding. Second, calculations of the thermodynamic linkage between proton binding and OMTKY3 stability are possible because the pK_a values have been determined for all ionizable groups in native OMTKY3 that are titrating between pH 1.5 and pH 12.4 (*31*, *32*; Forsyth and Robertson, unpublished results). On the basis of these calculations, the unfolding of OMTKY3 between pH 6 and pH 10 is expected to be accompanied by very little proton uptake or release. This suggests that OMTKY3 stability and, presumably, k_{op} and k_{cl} are not changing much over this range of pH.

Native-state NH exchange monitored by 1D NMR has been used to determine k_{obs} for the 13 slowest exchanging NHs in OMTKY3. NH exchange for 10 of these NHs shows good agreement with independent measures of global unfolding (*20*), so the simple two-state model for exchange can be used to analyze the data. The other three NHs are Cys 38, Asn 39, and Ala 40, all of which show exchange that is slower than expected on the basis of OMTKY3 stability (*20*). Semilogarithmic plots of k_{obs} versus pH are shown in Figure 1 for all NHs except Asn 33, whose exchange is very similar to that of Asn 28.

For all residues, k_{obs} increases by a factor of 10 per pH unit between pH 6 and pH 8.5. This is consistent with EX2 exchange (eq 3): k_{obs} is a product of the equilibrium constant for opening (k_{op}/k_{cl}), which is largely insensitive to pH, and k_{ch}, which is proportional to the concentration of hydroxide ion (*10*). Above pH 8.5, the pH dependence of k_{obs} decreases and, in some cases, disappears. This is consistent with a

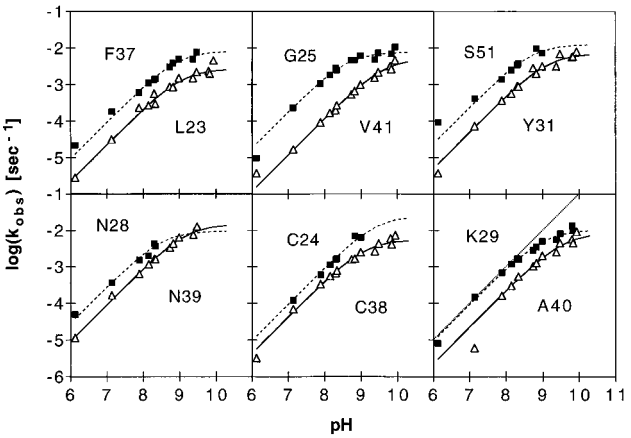

FIGURE 1: Semilogarithmic plots of the observed rate of exchange, k_{obs}, versus pH for 12 of the 13 NHs monitored in this study. To facilitate visualization of the general trend of the data, a dotted line with a slope of 1 has been added to the lower right panel next to the data for Lys 29. Using eq 2, observed rates for all NHs except Cys 24, Asn 28, and Asn 33 were subjected to nonlinear regression analysis (*30*). In order to eliminate fitting bias caused by larger observed rate constants at high pH, k_{obs} values have been weighted by the reciprocal of their magnitude normalized to the slowest exchange rate at a specific site. Results of the fits are reported in Table 1. The plateau values for Cys 24, Asn 28, and Asn 33 (data not shown) were insufficient for fitting, so simulations of eq 2 were used to obtain lower limits for k_{op} and k_{cl}. Solid and dashed lines represent the fitted or simulated curves for each NH group.

Table 1: Values for k_{op} and k_{cl} for Native OMTKY3 at 30 °C[a]

residue	$10^2 k_{op}$ (s^{-1})	k_{cl} (s^{-1})	$\Delta G°$ [c] (kcal/mol)
Leu 23	0.3 (0.1, 0.6)	2.1 (0.6, 7.7) × 10^2	6.7
Cys 24[b]	>2.5	>6.3 × 10^3	7.5
Gly 25	0.8 (0.5, 1.1)	2.5 (1.2, 5.5) × 10^3	7.7
Asn 28[b]	>1.0	>7.5 × 10^2	7.0
Lys 29	1.0 (0.6, 1.8)	2.4 (0.9, 6.3) × 10^3	7.4
Tyr 31	0.7 (0.4, 1.3)	1.3 (0.5, 3.8) × 10^3	7.3
Asn 33[b]	>2.8	>2.3 × 10^3	6.9
Phe 37	0.8 (0.4, 1.8)	1.2 (0.4, 3.8) × 10^3	7.1
Cys 38	0.6 (0.3, 1.0)	5.8 (2.3, 16) × 10^3	8.4
Asn 39	1.5 (0.6, 4.8)	1.5 (0.5, 7.2) × 10^4	8.3
Ala 40	0.8 (0.4, 3.0)	8.5 (2.8, 48) × 10^3	8.4
Val 41	0.5 (0.3, 1.0)	9.7 (4.8, 23) × 10^2	7.3
Ser 51	1.3 (0.4, 15)	0.8 (0.2, 18) × 10^3	6.7

[a] Values for all residues except Cys 24, Asn 28, and Asn 33 were determined from nonlinear regression analysis using eq 2. Numbers in parentheses denote lower and upper limits corresponding to a 95% confidence level. The fitting error was determined using *F* analysis (*44*). [b] Simulations of eq 2 were used to obtain lower limits for Cys 24, Asn 28, and Asn 33. [c] Estimated error for $\Delta G°$ is 0.5 kcal/mol (*20*).

switch in the rate-limiting step for NH exchange to the opening reaction (i.e., EX1 exchange), in which case the plateau value of k_{obs} approaches the opening rate, k_{op}. Values for k_{op} and k_{cl} at 10 of the 13 NHs have been obtained by nonlinear least-squares fitting of the data in Figure 1 to eq 2. Plateau regions for Cys 24, Asn 28, and Asn 33 (data not shown) were insufficiently defined for fitting, so simulations of eq 2 were used to obtain lower limits for k_{op} and k_{cl} (Table 1).

For some NHs, the plateaus in Figure 1 appear to be represented by very few data points. In fact, the curvature in most of these plots begins below the pH at which the plateau is evident. This is illustrated in the lower right panel of Figure 1, where a dotted line with a slope of 1 has been superimposed on the fitted curve for Lys 29. The data show systematic deviations from a unit slope as low as pH 8, and these deviations are well described by the fitted curve.

The k_{op} values obtained by least-squares analysis vary by less than an order of magnitude, ranging from 0.003 to $\geq$0.028 s^{-1} (Table 1). At the extremes, the differences in k_{op} values are significant, but many of the k_{op} values overlap at the 95% confidence level. However, the k_{op} values for Cys 24 and Asn 33 must be at least twice the fastest rate obtained from the fits, so the overall range of k_{op} values covers at least an order of magnitude.

The k_{cl} values appear to cover a wider range than is seen for k_{op}. The fitted k_{cl} values vary by nearly 2 orders of magnitude, ranging from 200 to 15000 s^{-1} (Table 1). Solid and dashed lines represent the fitted or simulated curves for each NH group (Figure 1). Overall, the fitted curves intersect the data well, which further suggests that the two-state NH exchange model (eq 1) is sufficient to describe the exchange behavior of the most slowly exchanging NHs in OMTKY3.

Some of the 95% confidence intervals reported in Table 1 cover more than an order of magnitude in rate constant. The magnitude of this uncertainty is directly related to the extent to which the pH-independent plateau is described by the data (Figure 1). This, in turn, is a function of the relative magnitudes of k_{cl} and k_{ch} (eq 2), at the highest pH where exchange was measured. To illustrate this relationship, the data for Gly 25 in Figure 1 have been subjected to a systematic series of truncations, starting at high pH, followed by least-squares analysis; for the complete data set, k_{ch} at the highest experimental pH is about 20 times the fitted value of k_{cl}. The k_{cl} value and 95% confidence interval for truncated data sets are equal to those for the complete data set until k_{ch} is about two or three times the fitted k_{cl} value. In general, the residues with the largest confidence intervals in Table 1, Asn 39, Ala 40, Val 41, and Ser 51, are also those where the largest k_{ch} value is only about two times the fitted k_{cl} value.

Kinetics of the opening and closing reactions at individual NHs have been mapped onto the three-dimensional structure of OMTKY3 in Figure 2. All 13 residues monitored in this study reside within regions of secondary structure. Opening rates are fairly uniform throughout the α-helix and β-sheet. The clear exceptions are Cys 24, which is hydrogen bonded to the third strand of the β-sheet, and Asn 33, the first residue of the helix, both of which open almost three times faster than any other residue. The slowest opening occurs at Leu 23, which is hydrogen bonded to Tyr 31 and located at the juncture between the helix and sheet.

Closing rates vary widely throughout OMTKY3 and even within individual secondary structures. The most rapid closure occurs in the middle of the helix at Cys 38, Asn 39, and Ala 40, where time constants (τ) range from 70 to 170 μs. Interestingly, exchange at these NHs was previously observed to be slower than expected on the basis of OMTKY3 stability (*20*). One hypothesis to explain this very slow exchange is residual nonrandom structure in the denatured state (*20*), so perhaps the observed kinetics are those for formation of structure in the denatured state. Rapid folding also takes place in the middle strand of the β-sheet at Cys 24 ($\tau \leq 160$ μs). Intermediate closing rates are found in the remainder of the helix and most of the sheet (τ values range from 400 to 1200 μs), while the slowest folding occurs at the juncture between the helix and sheet at Leu 23 ($\tau \approx$ 5000 μs).

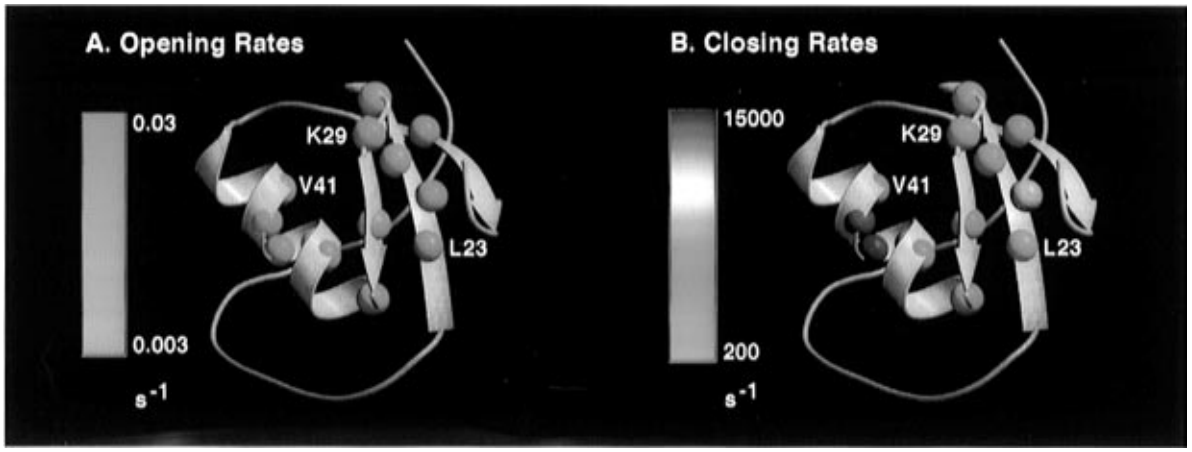

FIGURE 2: Kinetics of opening (A) and closing (B) reactions at individual NHs mapped onto the three-dimensional structure of OMTKY3 (*45*, *46*). Opening and closing rates from Table 1 have been color-coded and superimposed on balls representing individual NHs.

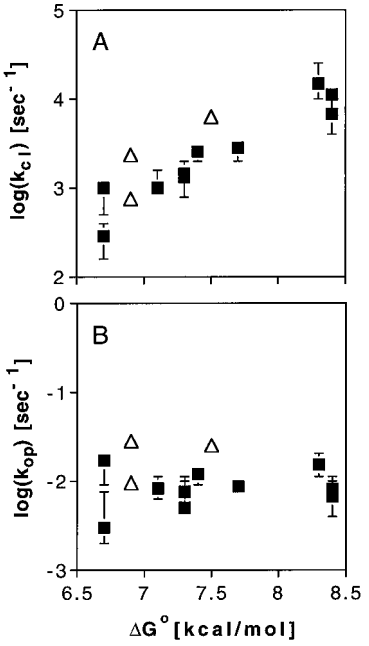

FIGURE 3: Closing (A) and opening (B) rates versus free energy. Free energies were determined from exchange-derived equilibrium constants (k_{op}/k_{cl}). Opening and closing rates are those presented in Table 1 (rates for Cys 24, Asn 28, and Asn 33 are lower limits obtained from simulations and are denoted by open triangles). The error bars are fitting errors at 1 SD; lack of an error bar means that it is obscured by the symbol.

The free energy of the opening reaction can be determined by NH exchange in the EX2 limit (eq 3):

$$\Delta G^\circ = RT \ln(k_{op}/k_{cl}) \quad (6)$$

Plots of this free energy versus $\log(k_{cl})$ and $\log(k_{op})$ (Figure 3) reveal that stability at any given NH correlates best with k_{cl} (Figure 3B); i.e., the NHs with the most rapid closing kinetics are generally those that are most stable to exchange in native OMTKY3. A number of groups have either proposed or observed such a relationship for other proteins (*21*, *33*, *34*). Some investigators have pointed out that observation of such a relationship is "purely fortuitous" because no *a priori* relationship exists between equilibrium distributions of species and the kinetics of interconversion among these species (*16*).

DISCUSSION

The fitted values of k_{op} are derived from the curvature and plateaus described by the data in Figure 1 and are thus directly related to the experimental observables. Most of the k_{op} values overlap at the 95% confidence level, but significant differences are observed between the slowest and most rapid rates, 0.003 s^{-1} at Leu 23 and $\geq$0.025 s^{-1} at Cys 24 and Asn 33 (Table 1, Figure 3B). This order of magnitude difference in opening rates is at odds with our previous conclusions regarding exchange at these sites: the similarity in ΔG° values to one another and to that for unfolding had led us to conclude that these NHs were exchanging by global unfolding (*20*). However, the real differences in k_{op} values clearly demonstrate that these three NHs cannot be reporting on the same molecular events. Nevertheless, the fact that k_{op} for Leu 23 is similar to values for the other 10 NHs is consistent with an exchange mechanism whereby the bulk of the slowly exchanging NHs exchange at the same molecular fluctuation, which is presumably global unfolding of OMTKY3.

Fitted values of k_{cl} depend entirely on knowledge of k_{ch}: a 3-fold increase in k_{ch}, for example, results in a 3-fold increase in k_{cl}. In this regard, predicted values of k_{ch} generally agree to within a factor of 3 with rates observed in denatured proteins (*35*−*40*). In addition, exchange rates in OMTKY3 peptide fragments, including those containing disulfide bonds, have been found to coincide with predicted k_{ch} values (Bowers, Rubach, and Robertson, unpublished results); the largest discrepancy between measured and predicted k_{ch} is a factor of 3, and most of the measured and predicted values are within a factor of 2. Additional evidence for the accuracy of predicted k_{ch} values in OMTKY3 is the good agreement between the equilibrium measurements of unfolding made with NH exchange and calorimetry (*20*). Overall, k_{ch} values for NHs that exchange by complete unfolding appear to be predicted accurately from the model compound values, which results in an uncertainty of no more than a factor of 3 in k_{cl} or about 0.5 kcal/mol in free energy.

One interesting result with respect to previous studies of OMTKY3 is the wide spread in ΔG° values, 6.7−8.4 kcal/mol, for the 13 slowest exchanging NHs in OMTKY3 (Table 1). The three NHs with the largest ΔG° values are a distinct set, whose ΔG° values of 8.3−8.4 kcal/mol are at least 0.6 kcal/mol greater than the next largest value (Table 1, Figure

3). These three NHs are the "superprotected" NHs identified previously (*20*).

The remaining 10 NHs have $\Delta G°$ values evenly distributed between 6.7 and 7.7 kcal/mol. The free energy of unfolding for OMTKY3 under these conditions is 7.1 (±0.5) kcal/mol (*31*; Forsyth and Robertson, unpublished results). The free energies in Table 1 are very similar to those obtained previously at pH 5 and 30 °C (see Figures 5 and 6 in ref *20*). Thus the distribution of $\Delta G°$ values is the result of significant systematic differences and not random error. Two possible explanations for the spread in $\Delta G°$ are (1) that there are inaccuracies in k_{ch} (see above) or (2) the $\Delta G°$ values are accurate and reflect real heterogeneity in the microscopic behavior at individual NHs in OMTKY3. The latter result is consistent with the observed heterogeneity in k_{op} values. In addition, Hilser and Freire (*41*) predict heterogeneous $\Delta G°$ values in their statistical thermodynamic model of NH exchange from native proteins.

How appropriate is the two-state mechanism (eq 1) for the interpretation of these studies? In other words, is there any evidence that more than one conformational equilibrium may be contributing to exchange at any given NH? For the slowest exchanging NHs in OMTKY3, exchange is predominantly mediated by a complete or nearly complete unfolding event (*20*), and the similarity of most k_{op} values is consistent with this interpretation: excluding Cys 24, Asn 28, and Asn 33, the mean k_{op} value is 0.008 (±0.004) s^{-1}. The results for Cys 24, Asn 28, and Asn 33 suggest that, in contrast to most slowly exchanging NHs in OMTKY3, these residues are undergoing EX2-type exchange at pH >8.5; i.e., they are exchanging at fluctuations occurring more rapidly than global unfolding. Thus, exchange at these residues may include contributions from both global and more local structural fluctuations. More generally, the simple two-state model is probably not appropriate for more rapidly exchanging NHs, where multiple equilibria are likely to contribute to the exchange behavior (*11*, *12*, *20*, *41*).

Knowledge of the extent to which exchange at different NHs may be monitoring the same structural events would provide valuable insight into the molecular events in unfolding and folding. Formally, exchange rates alone provide no information about correlations between neighboring NHs. However, patterns in rates and structural locations suggest that multiple NHs may be reporting on the same or related conformational changes during unfolding and folding. For example, most of the NHs in this study exchange when the protein is unfolded, so the narrow distribution of k_{op} values (Table 1) suggests that unfolding at these NHs is nearly (but not quite) an all-or-none event. Similar behavior was observed in the unfolding of ribonuclease A (*27*).

If unfolding of OMKTY3 were indeed an all-or-none process, then initiation of the folding reaction at the different NHs would be synchronized, in which case the hierarchy of k_{cl} values and the tendency of similar values to cluster within the structure would reflect an order of events in folding. On the other hand, an exchange rate may reflect the statistical probability that a particular residue is involved in structure rather than a discrete order of events during folding (*5*, *41*, *42*) and the structural coincidences reflect the tendencies of neighboring residues to participate in similar structures. In truth, the exchange data in this study contain no *direct* information regarding correlated events at different NHs. This information will have to come from additional NMR and mass spectrometry experiments (*23*, *25*, *26*).

Native-state NH exchange provides unprecedented access to structural information on a microsecond time scale. The early events in OMTKY3 folding correspond in time to the "burst phase" observed in many stopped-flow and quenched-flow studies, where structural changes are occurring in the millisecond dead times. Many proteins which undergo a two-state folding reaction fold in 20 ms or less, and rapid folding may go to completion with time constants as low as 100 μs (*6*). Suggested diffusion-limited time constants for elementary events in folding include about 0.1 μs for nucleating a helix (*43*), 0.5 μs for forming a turn, and about 1 μs for forming a 6−10 residue loop (*6*). OMTKY3 is refractory to chemical denaturation at temperatures below 40 °C, so direct measures of the overall kinetics of unfolding and refolding are not readily feasible; the slowest folding observed by native-state exchange is at Leu 23, whose time constant of 5 ms should put a lower limit on the kinetics for the overall folding reaction.

Folding kinetics for Cys 38, Asn 39, and Ala 40, which probably report on formation of a helical turn, are about 2 orders of magnitude slower than the proposed diffusion limit. Likewise, formation of the hairpin in the β-sheet, as monitored by Leu 23 and Tyr 31, is slowed by a factor of ≥1000 relative to the diffusion limit. These results suggest the presence of kinetic barriers to helix and sheet formation during the very early stages of folding in OMTKY3. The nature of these barriers can be explored by varying denaturant concentration and temperature.

Access to very rapid kinetics via native-state NH exchange entails systematic measurements of exchange under conditions where both equilibria and opening rates are assessed. In the present study, pH has been varied to change the rate-limiting step in NH exchange from the chemical step to the conformational opening reaction. Alternatively, chemical denaturants or temperature might be used to achieve similar ends (*12*, *26*). The beauty of pH as a variable is the characteristic plateau effect at alkaline pH (Figure 1) which permits identification of EX1-type exchange conditions. Interpretation of studies where pH is the perturbant will be facilitated by knowledge of the pH dependence of stability. In addition, error analysis in the present study suggests that reliable estimates for k_{op} and k_{cl} require that the experimental pH be extended to the point where k_{ch} is at least two or three times k_{cl}. Studies involving other perturbants will need to use other techniques to determine when EX1-type exchange is being observed (*23*, *25*, *26*).

More generally, native-state NH exchange may be used to measure the kinetics of conformational changes in addition to the unfolding and folding reactions. Possible applications include the study of conformational changes associated with binding, allosteric regulation, and rate-limiting steps in enzyme catalysis.

ACKNOWLEDGMENT

We thank members of the Robertson laboratory, Dr. Kenneth P. Murphy and Dr. Robert L. Baldwin for helpful discussions and comments on the manuscript. We also thank Dr. Liskin Swint-Kruse for generous assistance in the initial stages of this study.

REFERENCES

1. Roder, H., and Wüthrich, K. (1986) *Proteins 1*, 34−42.
2. Huang, G. S., and Oas, T. G. (1995) *Proc. Natl. Acad. Sci. U.S.A. 92*, 6878−6882.
3. Nolting, B., Golbik, R., and Fersht, A. R. (1995) *Proc. Natl. Acad. Sci. U.S.A. 92*, 10668−10672.
4. Schindler, T., and Schmid, F. X. (1996) *Biochemistry 35*, 16833−16842.
5. Dill, K. A., and Chan, H. S. (1997) *Nat. Struct. Biol. 4*, 10−19.
6. Eaton, W. A., Muñoz, V., Thompson, P. A., Chan, C. K., and Hofrichter, J. (1996) *Curr. Opin. Struct. Biol. 7*, 10−14.
7. Baldwin, R. L. (1993) *Curr. Opin. Struct. Biol. 3*, 84−91.
8. Woodward, C. K. (1994) *Curr. Opin. Struct. Biol. 4*, 112−116.
9. Hvidt, A. (1964) *C. R. Trav. Lab. Carlsberg 34*, 299−317.
10. Bai, Y., Milne, J. S., Mayne, L., and Englander, S. W. (1993) *Proteins 17*, 75−86.
11. Qian, H., Mayo, S. L., and Morton, A. (1994) *Biochemistry 33*, 8167−8171.
12. Loh, S. N., Rohl, C. A., Kiefhaber, T., and Baldwin, R. L. (1996) *Proc. Natl. Acad. Sci. U.S.A. 93*, 1982−1987.
13. Roder, H. (1989) *Methods Enzymol. 176*, 446−473.
14. Kim, K. S., Fuchs, J. A., and Woodward, C. K. (1993) *Biochemistry 32*, 9600−9608.
15. Loh, S. N., Prehoda, K. E., Wang, J., and Markley, J. L. (1993) *Biochemistry 32*, 11022−11028.
16. Clarke, J., and Fersht, A. R. (1996) *Folding Des. 1*, 243−254.
17. Bai, Y., Milne, J. S., Mayne, L., and Englander, S. W. (1994) *Proteins 20*, 4−14.
18. Orban, J., Alexander, P., Bryan, P., and Khare, D. (1995) *Biochemistry 34*, 15291−15300.
19. Perrett, S., Clarke, J., Hounslow, A. M. and Fersht, A. R. (1995) *Biochemistry 34*, 9288−9298.
20. Swint-Kruse, L., and Robertson, A. D. (1996) *Biochemistry 35*, 171−180.
21. Chamberlain, A. K., Handel, T. M., and Marqusee, S. (1996) *Nat. Struct. Biol. 3*, 782−787.
22. Hilton, B. D., and Woodward, C. K. (1979) *Biochemistry 18*, 5834−5841.
23. Roder H., Wagner, G., and Wüthrich, K. (1985) *Biochemistry 24*, 7396−7407.
24. Pedersen, T. G., Thomsen, N. K., Andersen, K. V., Madsen, J. C., and Poulsen, F. M. (1993) *J. Mol. Biol. 230*, 651−660.
25. Yi, Q., and Baker, D. (1996) *Protein Sci. 5*, 1060−1066.
26. Miranker, A., Robinson, C. V., Radford, S. E., Aplin, R. T., and Dobson, C. M. (1993) *Science 262*, 896−900.
27. Kiefhaber, T., and Baldwin, R. L. (1995) *Proc. Natl. Acad. Sci. U.S.A. 92*, 2657−2661.
28. Tanford, C. (1970) *Adv. Protein Chem. 24*, 1−95.
29. Van Geet, A. L. (1968) *Anal. Chem. 40*, 2227−2229.
30. Johnson, M. L., and Faunt, L. M. (1992) *Methods Enzymol. 210*, 1−37.
31. Swint-Kruse, L., and Robertson, A. D. (1995) *Biochemistry 34*, 4724−4732.
32. Schaller, W., and Robertson, A. D. (1995) *Biochemistry 34*, 4714−4723.
33. Woodward, C. (1993) *Trends Biochem. Sci. 18*, 359−360.
34. Bai, Y., Sosnick, T. R., Mayne, L., and Englander, S. W. (1995) *Science 269*, 192−197.
35. Roder H., Wagner, G., and Wüthrich, K. (1985) *Biochemistry 24*, 7407−7411.
36. Robertson, A. D., and Baldwin, R. L. (1991) *Biochemistry 30*, 9907−9913.
37. Lu, J., and Dahlquist, F. W. (1992) *Biochemistry 31*, 4749−4756.
38. Radford, S. E., Buck, M., Topping, K. D., Dobson, C. M., and Evans, P. A. (1992) *Proteins 14*, 237−248.
39. Arcus, V. L., Vuilleumier, S., Freund, S. M. V., Bycroft, M., and Fersht, A. R. (1994) *Proc. Natl. Acad. Sci. U.S.A. 91*, 9412−9416.
40. Buck, M., Radford, S. E., and Dobson, C. M. (1994) *J. Mol. Biol. 237*, 247−254.
41. Hilser V. J., and Freire, E. (1996) *J. Mol. Biol. 17*, 756−772.
42. Bryngelson, J. D., Onuchic, J. N., Socci, N. D., and Wolynes, P. G. (1995) *Proteins 21*, 167−195.
43. Gruenewald, B., Nicola, C. U., Lustig, A., Schwarz, G., and Klump, H. (1979) *Biophys. Chem. 9*, 137−147.
44. Bevington, P. R., and Robinson, D. K. (1992) *Data Reduction and Error Analysis for the Physical Sciences*, McGraw-Hill Book Co., New York.
45. Bode, W., Epp, O., Huber, R., Laskowski, M., and Ardelt, W. (1985) *Eur. J. Biochem. 147*, 387−395.
46. Kraulis, P. J. (1991) *J. Appl. Crystallogr. 24*, 946−950.

BI970872M